Magnetic Resonant Coupling As a Potential Means for Wireless Power Transfer to Multiple Small Receivers

Benjamin L. Cannon, *Student Member, IEEE*, James F. Hoburg, *Fellow, IEEE*, Daniel D. Stancil, *Fellow, IEEE*, and Seth Copen Goldstein, *Senior Member, IEEE*

***Abstract*—Wireless power transfer via magnetic resonant coupling is experimentally demonstrated in a system with a large source coil and either one or two small receivers. Resonance between source and load coils is achieved with lumped capacitors terminating the coils. A circuit model is developed to describe the system with a single receiver, and extended to describe the system with two receivers. With parameter values chosen to obtain good fits, the circuit models yield transfer frequency responses that are in good agreement with experimental measurements over a range of frequencies that span the resonance. Resonant frequency splitting is observed experimentally and described theoretically for the multiple receiver system. In the single receiver system at resonance, more than 50% of the power that is supplied by the actual source is delivered to the load. In a multiple receiver system, a means for tracking frequency shifts and continuously retuning the lumped capacitances that terminate each receiver coil so as to maximize efficiency is a key issue for future work.**

***Index Terms*—Microrobotics, resonant coupling, swarm robotics, wireless power.**

I. Introduction

An efficient method for wireless power transfer would enable advances in such diverse areas as embedded computing, mobile computing, sensor networks, and microrobotics. The need to minimize energy consumption is often the main design driver in applications where devices need to operate untethered. Energy consumption often restricts or severely limits functionality in such applications.

The work described in this paper is motivated by potential application of magnetic resonant coupling as a means for wireless power transfer from a source coil to multiple receivers. Through simple experimental setups and corresponding circuit models, we address issues that are involved in applying the basic mechanism to both a single receiver and multiple receivers with sizes much smaller than the source coil.

Manuscript received December 18, 2008; revised February 17, 2009. Current version published July 31, 2009. Recommended for publication by Associate Editor B. Ferreira.

B. L. Cannon was with the Department of Electrical and Computer Engineering, Carnegie Mellon University, Pittsburgh, PA 15213 USA. He is now with the Department of Electrical Engineering and Computer Science, Massachusetts Institute of Technology, Cambridge, MA 02139 USA (e-mail: bcannon@mit.edu).

J. F. Hoburg and D. D. Stancil are with the Department of Electrical and Computer Engineering, Carnegie Mellon University, Pittsburgh, PA 15213 USA (e-mail: hoburg@ece.cmu.edu; stencil@ece.cmu.edu).

S. C. Goldstein is with the Department of Computer Science, Carnegie Mellon University, Pittsburgh, PA 15213 USA (e-mail: seth@cs.cmu.edu).

Color versions of one or more of the figures in this paper are available online at http://ieeexplore.ieee.org.

Digital Object Identifier 10.1109/TPEL.2009.2017195

Inductive coupling is an old and well-understood method of wireless power transfer. The source drives a primary coil, creating a sinusoidally varying magnetic field, which induces a voltage across the terminals of a secondary coil, and thus transfers power to a load. This mechanism, responsible for power transfer in a transformer, where the magnetic field is typically confined to a high permeability core, also functions when the region between the primary and secondary coils is simply air. Inductive coupling without high permeability cores is used, for example, to power RF ID tags and medical implants [1]–[3]. A common technique for increasing the voltage received by the device to be powered is to add a parallel capacitor to the secondary to form a resonant circuit at the operating frequency [1], [2]. Application of this principle has also been demonstrated for powering robot swarms [4]. In this case, resonance was used on the primary but not on the secondary windings on the robots. This was done to minimize performance variations resulting from interactions among the robots. Recent work [5] has shown that when resonance is used on both the primary and secondary, power can be transferred with very little radiated loss and with 40%–50% of the source power delivered to the load, even when the secondary coil links only a relatively small part of the magnetic field that is created by the primary. A coupled-mode analysis of the interaction between a pair of resonant coils has also been presented [5], [6]. Finally, an inductively coupled radio frequency wireless transmission system has been described, with reference to multiple resonant peaks for multiple receivers [7].

In the work described here, there are two new contributions:

1) We demonstrate power transfer from a single resonant source coil to multiple resonant receivers, focusing upon the resonant frequency splitting issues that arise in multiple receiver applications.
2) We show that resonant coupling systems with either single or multiple receivers can be modeled using a relatively simple circuit description. The model rigorously takes into account mutual coupling between all coils, and does not make approximations usually associated with the coupled-mode approach [8]. This description makes it clear that high Q resonant coupling is key to the efficiency of the system, through an implementation where the primary coil is inductively coupled to the power source and the receiving coils are inductively coupled to the loads.

We expect this work to form a basis for understanding and extending the resonant coupling mechanism to multiple mobile receivers. The main challenge for such a system is to adjust the

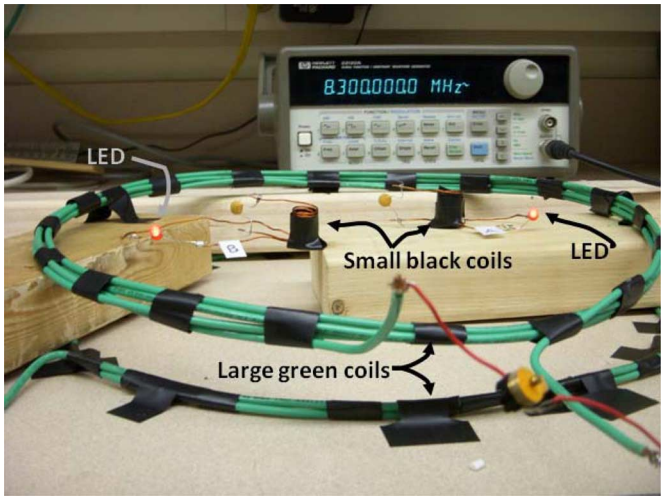

Fig. 1. Photograph of a signal generator wirelessly supplying power to two LEDs (tagged A and B) through magnetic resonant coupling between large (green) and small (black) coils. The signal generator drives the lower green coil, while lumped capacitors terminate the upper green coil and each of two small receiving coils, which in turn are inductively coupled to coils that drive the LEDs.

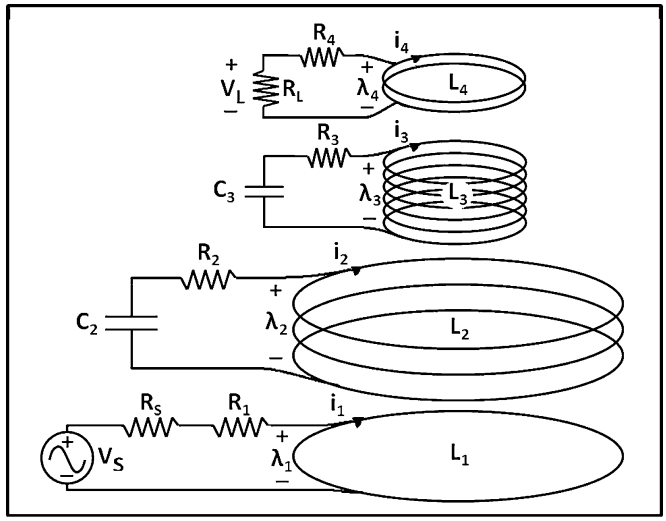

Fig. 2. A schematic circuit drawing of a source coil pair and a single-receiving coil pair. Each load in a multiple receiver system involves a receiving coil pair.

lumped capacitances at the terminals of the receivers as they move with respect to the source coil and with respect to one another.

II. Experimental Setup of a Resonant Coupled System With Two Loads

Fig. 1 shows a photograph of a resonant coupling system wherein a signal generator delivers power to two illuminated LEDs (tagged A and B). The source, operating at a resonant frequency of 8.3 MHz, is connected directly across the terminals of the lower of two large green coils with diameters of 30 cm, spaced 3.8 cm apart. The upper green coil is inductively coupled to the lower coil, and is terminated by an adjustable lumped capacitor (with red leads). In the center of the upper green coil are two small receivers, each of which consists of a coil with diameter 1.3 cm that is terminated by a lumped capacitor, inductively coupled to a separate coil with the same diameter that is terminated by an LED. The two coils in each of the two receivers are together wrapped in black electrical tape. The system thus involves a total of six coils, a "source coil pair" and a "receiving coil pair" for each of two receivers associated with the two loads. The fact that the source and loads are connected to coils that are inductively coupled to, but distinct from the coils that are terminated by lumped capacitances is key to establishing a high Q resonant coupling, with the resonant frequency determined by adjusting the lumped capacitances.

III. Circuit Representation of a Resonant Coupled System With a Single Load

Fig. 2 shows a schematic circuit representation of a system like the experimental system shown in Fig. 1, but with only a single load coil pair. We use this system to develop an understanding of the resonant coupling mechanism and to serve as a basis for extending it to multiple receivers. Our experimental results include measurements for both the two-receiver system that is shown in Fig. 1 and for a single-receiver system corresponding to the circuit representation shown in Fig. 2.

In the single-receiver system of Fig. 2, the source drives a large single-turn coil, labeled L_1 that is inductively coupled to a large multiturn resonant coil L_2 of the same diameter. The small resonant coil L_3 is inductively coupled to a small coil of the same diameter, labeled L_4, that is terminated by a load element. Lumped capacitors C_2 and C_3 respectively terminate the resonant coils L_2 and L_3. The resistances R_1, R_2, R_3, and R_4 are the small resistances of the coils themselves, while R_S is the internal resistance of the source, and R_L is the load resistance. (The LEDs in Fig. 1 are nonlinear elements, used to demonstrate wireless power transfer. Measurements and the corresponding circuit representation described here and in subsequent sections use a resistive load.)

The work described in [5] used two identical open-circuited "self-resonant" coils, with a resonant frequency based upon the distributed inductance and distributed capacitance of each coil. Here, with completely different source and receiver coils, the lumped capacitances are chosen so as to yield identical resonant frequencies,

$$\omega_0 = \frac{1}{\sqrt{L_2 C_2}} = \frac{1}{\sqrt{L_3 C_3}}. \tag{1}$$

This alteration provides a simple means to achieve resonant coupling between a large source coil and one or several small receiving coils.

IV. Circuit Analysis

A circuit model for the experimental setup with only one receiving coil pair driving a single load, as represented in Fig. 2, is based upon the application of Kirchhoff's voltage law around each of the four loops. The voltage at the terminals of each coil is described as the time rate of change of flux linkage. Λ_1 through

Λ_4 and i_1 through i_4 represent complex amplitudes of flux linkages and currents in each of the four coils; V_S represents the complex amplitude of the ideal voltage source. With resistances R_1 through R_4, R_S, and R_L, and capacitances C_2 and C_3, the circuit constraints at frequency ω are

$$V_S = (R_S + R_1)\, i_1 + j\omega\Lambda_1 \tag{2}$$

$$0 = R_2 i_2 + \frac{i_2}{j\omega C_2} + j\omega\Lambda_2 \tag{3}$$

$$0 = R_3 i_3 + \frac{i_3}{j\omega C_3} + j\omega\Lambda_3 \tag{4}$$

$$0 = (R_4 + R_L)\, i_4 + j\omega\Lambda_4. \tag{5}$$

Since each of the four coils is inductively coupled to the other three, the flux linkages are related to the currents by a symmetric 4×4 inductance matrix:

$$\begin{bmatrix} \Lambda_1 \\ \Lambda_2 \\ \Lambda_3 \\ \Lambda_4 \end{bmatrix} = \begin{bmatrix} L_{11} & M_{12} & M_{13} & M_{14} \\ M_{12} & L_{22} & M_{23} & M_{24} \\ M_{13} & M_{23} & L_{33} & M_{34} \\ M_{14} & M_{24} & M_{34} & L_{44} \end{bmatrix} \begin{bmatrix} i_1 \\ i_2 \\ i_3 \\ i_4 \end{bmatrix}. \tag{6}$$

For a known ideal source voltage V_S and known resistances, capacitances, and self inductances and mutual inductances, (2) to (5), with (6) substituted for the flux linkages, comprise four simultaneous equations that determine the currents i_1 through i_4, and thus the complex amplitude of the load voltage $V_L = -R_L i_4$. Since the system is linear, this analysis determines the transfer function based upon the source frequency, $|(V_L/V_S)(\omega)|$.

Extension of the circuit model to multiple loads, as for the experimental two-load system shown in Fig. 1, is straightforward, with six equations replacing four. More generally, extension to an arbitrary number of loads is described in Section VIII.

The use of a circuit model here is appropriate because, as described in [5], the interaction involves magnetoquasistatic field structures. Equivalently, we can compare radiated electromagnetic power with power dissipated in the resistances of the circuit model. The radiation resistance R_r of a coil with N turns and radius a, at source frequency f and corresponding free space wavelength $\lambda = c/f$ where $c = 3.00 \times 10^8$ m/s is [9]

$$R_r = 20 \left(\frac{2\pi}{\lambda}\right)^4 \left(\pi a^2 N\right)^2. \tag{7}$$

Coil 2, then has the largest radiation resistance, with value $R_{r2} = 8.7 \times 10^{-4}\ \Omega$, which is far too small in comparison with the ohmic resistance R_2 to be significant.

Unintended magnetic coupling with nearby objects is of far less significance than it would be at higher frequencies, with wavelengths on the scale of the transmitting coil.

V. Comparison of Circuit Model With Experimental Measurements With a Single Receiver

Methods of determination and values for the various parameters in the circuit model described in Sections III and IV are given in the Appendix. Resistances, capacitances, and self-inductances are calculated values, while the coupling coefficients that determine mutual inductances are chosen so as to fit the theoretical model to the experimental frequency response of the system. Fig. 3 shows a theoretical curve based upon the circuit model for a set of coupling coefficients that yields a good fit, along with experimental data points on a power decibel scale.

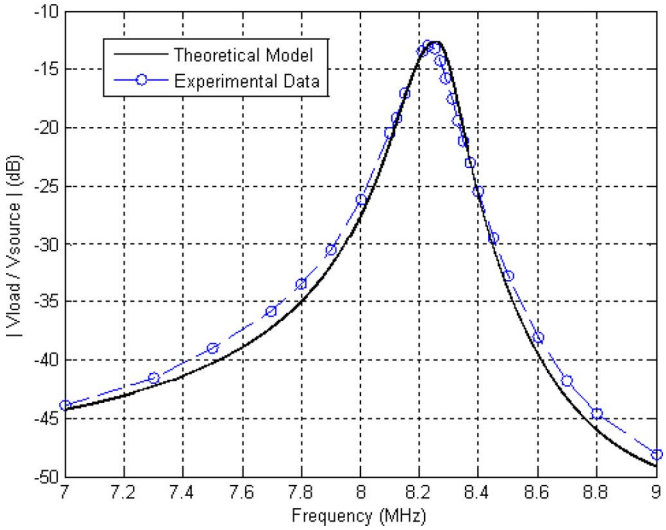

Fig. 3. Transfer function $|(V_L/V_S)(\omega)|$ near the resonant peak as measured experimentally and as calculated from the circuit model for the resonant coupled system with a single receiver.

It is apparent from Fig. 3 that the circuit model, with appropriately chosen parameter values, accurately describes the measured behavior of the resonant coupled system with a single receiver. It is likely that a robust minimization algorithm could be used to obtain even better agreement, but derivation of the coupling coefficients from first principles and refinement of the calculations of resistances, capacitances, and self-inductances are goals of ongoing work.

VI. Efficiency and Evaluation of Power Losses With a Single Receiver

For the experimental setup with a single receiver, the rms voltage across a 100-Ω resistive load placed in the center of the transmitting coil is 1.68 V, corresponding to a wireless delivered power of 28.2 mW. When the receiver is displaced 17 cm away from and along the axis of the transmitting coil (about 1 coil radius), the voltage drops by about a factor of 3 to 0.57 V, corresponding to 3.3 mW power delivered.

The difference between supplied and received power for the system with a single receiver is accounted for in the circuit model through power dissipation in the resistances. For the parameter values listed in the Appendix, 51.4% of the power that leaves the terminals of the actual source (ideal source in series with internal resistance R_S) is delivered to the load resistance R_L.

The percentages of the total power that is supplied by the ideal source V_S for the single-receiver system are:

1) 9.1% to load resistance R_L;
2) 82.3% to internal source resistance R_S;
3) 0.1% to source coil resistance R_1;
4) 6.8% to primary coil resistance R_2;

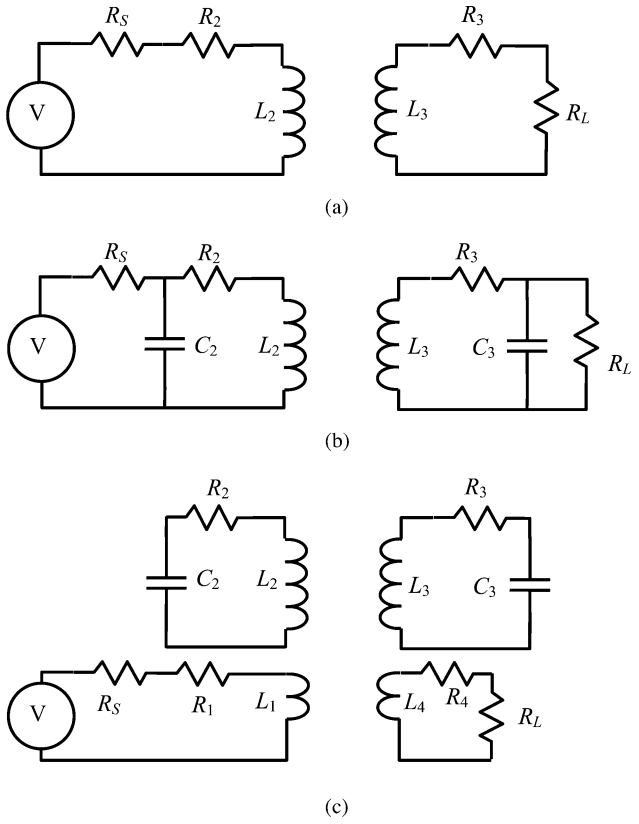

Fig. 4. Circuits illustrating nonresonant and resonant coupling. (a) Nonresonant inductive coupling. (b) Resonant coupling with significant loading by the source and load, resulting in low Q. (c) Resonant coupling with source and load inductively coupled to the resonant circuits in such a way as to reflect high parallel impedances, resulting in a high Q.

5) 1.7% to secondary coil resistance R_3;
6) 0.0% to load coil resistance R_4.

Thus, the dominant loss occurs in the internal source resistance R_S. This loss occurs whenever a source delivers power to a load, whether through wires or through a wireless power transfer method. (The high internal resistance of the function generator, used here only for concept demonstration, can be significantly reduced by using a more practical power source.) More than half of the remaining power is delivered to the load resistance R_L, with dissipation in the primary coil resistance R_2, the largest loss beyond the actual source terminals. The degree to which resistive losses can be reduced from the simple demonstration setup described here is a subject of our ongoing work.

VII. Comparison With Frequency Response for Simple Inductive Coupling

The circuit model provides a simple way to understand what is accomplished by the resonant coupling mechanism and how it differs from simple inductive coupling. Fig. 4 shows three circuits providing inductive coupling to the load. Fig. 4(a) shows simple nonresonant coupling, while (b) and (c) shows variations of resonant coupling. In Fig. 4(b), the source and load resistances are approximately in parallel with parallel *LC* resonant circuits if the ohmic resistances R_2, R_3 are small. Here the circuit Q is determined by the loading provided by R_S, R_L. In contrast, in Fig. 4(c), which corresponds to the system described in this paper, the source and load impedances are inductively coupled to the resonant circuits. In this case, the turns ratios can be chosen so that R_S, R_L are transformed into much larger effective resistances in parallel with the *LC* resonant circuits, resulting in a larger Q. Fig. 5 shows $|(V_L/V_S)(\omega)|$ as computed using these circuit models and component values appropriate for our experiment, as given in the Appendix. For the case of simple inductive coupling [Fig. 4(a)], the transfer function is almost constant at -58 dB for frequencies between 1 and 10 MHz, with low and high frequency 20 dB/decade roll-offs. For the values chosen, the Q of the circuit shown in Fig. 4(b) is relatively small, with only a weak resonant peak at a frequency that corresponds to ω_0. In contrast, the impedance transformation provided by the coupling coils L_1, L_4 for the circuit shown in Fig. 4(c) results in a much higher Q and coupling that is stronger by about 40 dB than the circuit shown in Fig. 4(b). Thus, the low Q and purely inductive systems have efficiencies many orders of magnitude lower than the high Q system.

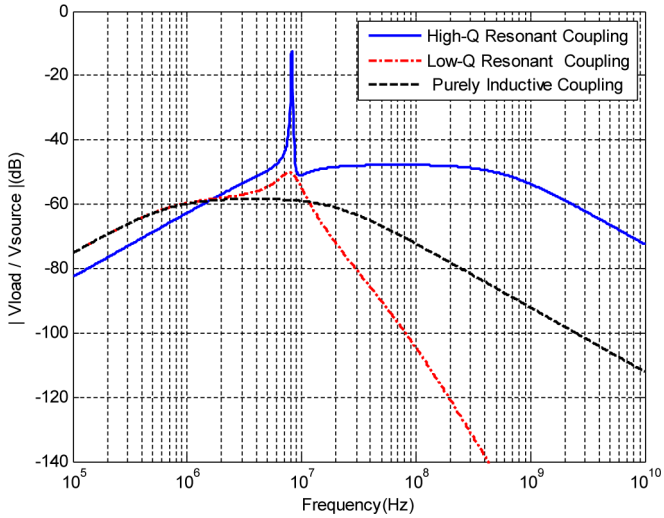

Fig. 5. Transfer function $|(V_L/V_S)(\omega)|$ over a wide frequency range from the circuit model for the resonant coupled system, and for two simple systems that connect the source and load directly to the coupled coils.

VIII. Delivery of Power to Multiple Loads

Wireless power delivery to multiple small receivers is simply a replication for each receiver of the principle that has been demonstrated and modeled in the prior sections of this paper, provided that two conditions are met.

1) Each receiver must carry small coils that remain within the region of relatively uniform magnetic field generated by the source coil.
2) Each receiver must be far enough separated from each other receiver that their interactions with the source coil are decoupled. Said another way, mutual inductances between the receiving coils must have a negligible effect upon the resonant coupling interaction.

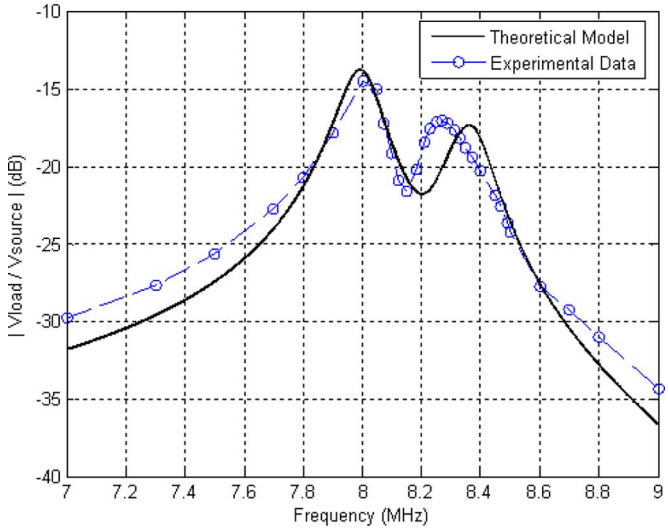

Fig. 6. Transfer function $|(V_L/V_S)(\omega)|$ near the resonant peak as measured experimentally and as calculated from the circuit model for two identical receiving coils stacked directly on top of one another in the center of the transmitting coil pair, so as to maximize the coupling interaction between receivers. Coupled mode splitting of the resonant peak is apparent.

The second of these conditions is likely to be repeatedly violated if the receivers move (for example, if they are microrobots). For this reason, we explore in this section the effect of bringing two receivers into close proximity. Coupled mode theory [7] predicts a splitting of the single-transfer function resonant peak into two separate peaks. Fig. 6 shows the measured transfer function across one of the two load resistors for two receiver coil pairs, each identical to the single coil pair that is described in prior sections, when the coils are stacked directly on top of one another in the center of the transmitting coil pair, so as to maximize the coupling interaction between receivers. The coupling between the two receivers in this case is stronger than in Fig. 1, where the receivers are side by side. Here, the single peak has split into two peaks, separated in frequency by about 3% of the original resonant frequency.

Also shown in Fig. 6 is a theoretical curve deriving from an extension of the circuit model to include two pairs of load coils, with coupling coefficients again chosen by using rough estimates of the fractions of magnetic flux from each coil that link each other coil, with adjustments in values so as to obtain a good overall fit of the circuit model to the experimental measurement. The circuit model clearly shows the same qualitative behavior with regard to frequency splitting.

As with the single receiver coil pair, our ongoing work involves determination of all parameter values for multiple receivers from first principles. The complexity of the circuit model grows quadratically with the number of receivers.

Of considerable interest for application of magnetic resonant coupling to wireless power transfer to multiple receivers is the degree to which frequency splitting degrades the efficiency of the interaction, and practical means for dealing with this potential difficulty. For example, it may be possible, through onboard control systems, to continuously retune the lumped capacitances that terminate each receiver coil so as to maximize efficiency. This area is a separate subject of our ongoing work.

IX. Summary

The following points have been demonstrated in this paper.

1) Magnetic resonant coupling can be used to deliver power from a large source coil to one or many small load coils, with lumped capacitors at the coil terminals providing a simple means to match resonant frequencies for the coils. This mechanism is a potentially robust means for delivering wireless power to multiple receivers from a single large-source coil.
2) A relatively simple circuit model describes the essential features of the resonant coupling interaction, with parameters that can be either derived from first principle descriptions, from direct measurement or from curve fitting techniques.
3) A key issue for powering of multiple receivers is the coupled mode frequency splitting that occurs when two receivers are in close enough proximity that their magnetic fields are relatively strongly coupled. Control circuitry to track the resonant frequency shifts and to retune the receiving coil capacitances is a potentially viable strategy for addressing this issue.

Appendix

Determination of Parameter Values

In principle, all the parameter values in the circuit model can be determined from first principles, based upon geometries and material parameters, and can be verified through individual measurements. While these calculations, as well as comparisons with direct measurements, are the subject of our ongoing work, our purpose here is simply to show that, using reasonable parameter values, the circuit model yields a frequency response description that is in good agreement with experimental measurements.

The parameter values in the circuit model are determined as follows:

1) *Coil Resistances* R_1, R_2, R_3, *and* R_4:
Skin effect causes the currents in the resonant coils to concentrate toward the surfaces of the copper wires, so that their effective areas are reduced from their cross-sectional areas. Thus, the resistances are described by

$$R = \frac{2\pi a N}{\sigma 2\pi r \delta} = \frac{aN}{\sigma r \delta} \tag{8}$$

with the following definitions of physical parameters:
a = major radius of coil ($a_1 = a_2 = 15$ cm, $a_3 = a_4 = 0.635$ cm)
r = cross-sectional radius of wire ($r_1 = r_2 = 1.5$ mm, $r_3 = r_4 = 0.45$ mm)
N = number of turns ($N_1 = 1, N_2 = 3, N_3 = 10.5, N_4 = 3$)
σ = copper conductivity ($\sigma = 5.8 \times 10^7$ S/m)
f = source frequency ($f = 8.3$ MHz)

$$\delta = \frac{1}{\sqrt{\pi f \mu_0 \sigma}} \text{ (skin depth) } (\delta = 22.9\ \mu\text{m})$$

$$\mu_0 = 4\pi \times 10^{-7}\ \text{H/m}$$

Equation (8) yields the following values for coil resistances at 8.3 MHz:

$$R_1 = 0.075\ \Omega, \qquad R_2 = 0.23\ \Omega$$

$$R_3 = 0.11\ \Omega, \qquad R_4 = 0.032\ \Omega$$

2) *Source Internal Resistance:* The HP 33120A Function/Arbitrary Waveform Generator has a manufacturer specified internal resistance:

$$R_S = 50\ \Omega.$$

3) *Load Resistance*: The load resistance is taken as the resistor color code value:

$$R_L = 100\ \Omega.$$

4) Self-inductance L_2 and capacitance C_2:
The coil L_2 was connected directly across the terminals of the function generator, and the frequency was adjusted so as to yield an amplitude of terminal voltage reduced by $1/\sqrt{2}$ from the open circuit voltage. At this frequency, the pure imaginary coil impedance has the same magnitude as the pure real source impedance of 50 Ω, so that $2\pi f L_2 = 50\ \Omega$. The measured frequency yields a self-inductance for coil 2 of

$$L_2 = 11.2\ \mu\text{H}.$$

A variable capacitor was used for C_2 so as to tune the resonance. Since its value was not directly available, the capacitance C_2 is determined from (1), with a resonant frequency $\omega_0 = 2\pi\,(8.3\ \text{MHz})$. (The value obtained in this way is actually the sum of C_2 and the distributed capacitance of the coil.) This yields the value:

$$C_2 = 34\ pF$$

5) Self-inductance L_3 and capacitance C_3: The capacitance C_3 is taken as the value printed on the lumped element:

$$C_3 = 470\ pF.$$

The inductance L_3 is then determined from (1), again with a resonant frequency $\omega_0 = 2\pi\,(8.3\ \text{MHz})$. (This value is an effective inductance that also includes the effects of the distributed capacitance of the coil.) This yields the value:

$$L_3 = 0.80\ \mu\text{H}.$$

6) Self-inductances L_1 and L_4: Since coils 1 and 4 are essentially identical respectively to coils 2 and 3, except that they have fewer turns, their self-inductances are inferred from L_2 and L_3 and the number of turns in the two resonant coils. Thus, using $L_1/L_2 = N_1^2/N_2^2$ and $L_4/L_3 = N_4^2/N_3^2$ yields the values:

$$L_1 = 1.2\ \mu\text{H}, \qquad L_4 = 0.065\ \mu\text{H}.$$

7) Mutual inductances $M_{12}, M_{13}, M_{14}, M_{23}, M_{24}$, and M_{34}: The mutual inductance between any pair of coils is proportional, through a coupling coefficient $\kappa \leq 1$ to the geometric mean of the two self-inductances [10]. Thus, the mutual inductances in (6) are represented in terms of coupling coefficients by

$$M_{ij} = \kappa_{ij}\sqrt{L_i L_j}. \tag{9}$$

Values for the six coupling coefficients $\kappa_{12}, \kappa_{13}, \kappa_{14}, \kappa_{23}, \kappa_{24}$, and κ_{34} are chosen by using rough estimates of the fractions of magnetic flux from each coil that link each other coil, and then by making small adjustments in values so as to fit the theoretical transfer function $|(V_L/V_S)(\omega)|$ to experimental data points over a range of frequencies that span the resonance. The specific values used are

$$\kappa_{12} = 0.17; \qquad \kappa_{13} = 0.0010; \qquad \kappa_{14} = 0.021;$$

$$\kappa_{23} = 0.0047; \qquad \kappa_{24} = 0.021; \qquad \kappa_{34} = 0.76.$$

REFERENCES

[1] K. Finkenzeller, *RFID Handbook: Fundamentals and Applications in Contactless Smart Cards and Identification*, 2nd ed. New York: Wiley, 2003, ch. 4.

[2] G. Wang, W. Liu, M. Sivaprakasam, M. Humayun, and J. Weiland, "Power supply topologies for biphasic stimulation in inductively powered implants," in *Proc. IEEE Int. Symp. Circuits Syst.* (ISCAS, 2005), vol. 3, no. 12, pp. 2743–2746.

[3] B. Jiang, J. R. Smith, M. Philipose, S. Roy, K. Sundara-Rajan, and A. V. Mamishev, "Energy scavenging for inductively coupled passive RFID systems," *IEEE Trans. Instrum. Meas.*, vol. 56, no. 1, pp. 118–125, Feb. 2007.

[4] T. Deyle and M. Reynolds, "Surface based wireless power transmission and bidirectional communication for autonomous robot swarms," in *Proc. IEEE Int. Conf. Robot. Autom.* (ICRA, 2008), pp. 1036–1041.

[5] A. Kurs, A. Karalis, R. Moffatt, J. D. Joannopoulos, P. Fisher, and M. Soljacic, "Wireless power transfer via strongly coupled magnetic resonances," *Science*, vol. 317, pp. 83–86, Jul. 6, 2007.

[6] A. Karalis, J. D. Joannopoulos, and M. Soljacic, "Efficient wireless non-radiative mid-range energy transfer," *Ann. Phys.*, vol. 323, no. 1, pp. 34–48, Jan. 2008.

[7] K. O'Brien, *Inductively Coupled Radio Frequency Power Transmission System for Wireless Systems and Devices*. Aachen, Germany: Shaker Verlag, 2007. ISBN 978-3-8322-5775-0.

[8] H. A. Haus, *Waves and Fields in Optoelectronics*. Englewood Cliffs, NJ: Prentice-Hall, 1984, pp. 197–234.

[9] J. D. Kraus, *Antennas*. New York: McGraw-Hill, 1988, p. 251.

[10] J. W. Nilsson and S. A. Riedel, *Electric Circuits*, 7th ed. Englewood Cliffs, NJ: Pearson Prentice-Hall, 2005, pp. 243–244.

Benjamin L. Cannon (S'08) received the B.S. degree in electrical and computer engineering from Carnegie Mellon University, Pittsburgh, PA, in 2008.

He is currently a Graduate Student in the Laboratory for Electromagnetic and Electronic Systems, Massachusetts Institute of Technology, Cambridge. His current research interests include electromagnetic sensors and electric and magnetic field interactions with materials.

James F. Hoburg (S'64–M'75–SM'85–F'01) received the B.S.E.E. degree in 1969 from Drexel University, Philadelphia, PA, and the S.M. and Electr. Eng. degrees in 1971 and the Ph.D. degree in 1975 from Massachusetts Institute of Technology, Cambridge.

He is currently a Professor of electrical and computer engineering at Carnegie Mellon University, Pittsburgh, PA. His current research interests include wide range of applications of engineering electromagnetics, including electric and magnetic field analysis and modeling, magnetic shielding, discrete and continuum electromechanical systems, applied electrostatics, electrohydrodynamics, and microfluidics.

Dr. Hoburg received the Ladd Award for excellence in research in 1979 and the Ryan Award for excellence in undergraduate teaching in 1980, both at Carnegie-Mellon.

Daniel D. Stancil (S'75–M'81–SM'91–F'01) received the B.S. degree in electrical engineering from Tennessee Technological University, Cookeville, in 1976, and the S.M., Electr. Eng., and Ph.D. degrees from Massachusetts Institute of Technology, Cambridge, in 1978, 1979, and 1981, respectively.

From 1981 to 1986, he was an Assistant Professor of electrical and computer engineering at North Carolina State University, Raleigh. In 1986, he joined the faculty at Carnegie Mellon University (CMU), Pittsburgh, PA, as an Associate Professor, and is currently a Professor of electrical and computer engineering. His current research interests include wireless communications and optical data storage.

Dr. Stancil received a Sigma Xi Research Award from North Carolina State University in 1985, and was a leader in the development of the CMU Electrical and Computer Engineering (ECE) Department's Virtual Laboratory, which was a finalist for a 1996 Smithsonian Computerworld Award. He was a co-recipient of the Science Award for Excellence in 1998 from the Pittsburgh Carnegie Science Center for the development and commercialization of electrooptics technology. In 1998, he was also recognized with an IR 100 Award and a Photonics Circle of Excellence Award for electrooptic scanning technology that he co-developed. He is a Past-President of the IEEE Magnetics Society.

Seth Copen Goldstein (M'96–SM'06) received the M.S. and Ph.D. degrees in computer science from the University of California, Berkeley, in 1994 and 1997, respectively.

He was with the Department of Electrical Engineering and Computer Science, Princeton University, for undergraduate work. He is currently an Associate Professor in the School of Computer Science, Carnegie Mellon University, Pittsburgh, PA. His current research interests include large collections of interacting agents. In the area of reconfigurable computing, he investigated how to compile high-level programming languages directly into configurations that could harness the large ensemble of gates for computing. Later work involved ensembles of molecules in the area of molecular electronics. This research investigated how to design, manufacture, and use molecular-scale devices for computing. He is currently involved in realizing Claytronics, a form of programmable matter.